Computational Prediction of the Low-Temperature Ferromagnetic Semiconducting 2D SiN Monolayer

Nikolay V. Tkachenko, Bingyi Song, Dmitriy Steglenko, Ruslan M. Minyaev, Li-Ming Yang, and Alexander I. Boldyrev*

Since the discovery of graphene, 2D materials have captured the minds of scientists because of their attractive and unique electronic properties. In particular, magnetic 2D materials have become a subject of extensive discussions today. Using density functional theory calculations, it is shown that 2D SiN sheet (built out of nonmetallic main group atoms) is a ferromagnetic semiconducting material with a magnetic moment $1\,\mu_B$ per unit cell and an indirect bandgap of 1.55 eV. Calculated phonon spectrum and conducted *ab initio* molecular dynamics simulation reveal thermal and dynamical stability of the designed material. It is shown that the ferromagnetic state is stable up to 20 K. Magnetism of silicon mononitride can be described by the presence of an unpaired electron located on silicon atoms. The semiconducting and ferromagnetic properties of SiN monolayer open many opportunities for its potential use in spintronic and nanoelectronic devices.

1. Introduction

Two-dimensional materials have been the subject of interest of the academic community over the years[1,2] due to the wide range of applications—from nanoelectronics[3,4] to data storage.[5] With the discovery of graphene,[6,7] methods for producing 2D materials continue to evolve. It has been already shown that the computational prediction of new materials with unimaginable properties[8–11] can set a direction for the experimenters who in subsequent works will find a way to synthesize these new materials. A typical example is the planar hexacoordinate Cu_2Si monolayer, which was predicted computationally in 2015[11] and, in just 2 years, fabricated experimentally.[12] Both experimental and theoretical results show fascinating properties. Furthermore, on the basis of electronic and geometric fits, a series of planar hypercoordinate monolayers have been predicted, such as, Cu_2Ge,[9] Ni_2Si/Ge,[10] Cu_2P/As,[13] and transition metal monolayers (Cu,[14] Ag,[15] Au,[16] Pt[17]). Quite recently, a brand-new 2D aluminum boride ($AlB_6-ptAl-$array) nanosheet with a planar tetracoordinate aluminum (ptAl) array was predicted to be a highly stable superconductive material with triple Dirac cones.[18] Now, a new class of 2D materials, planar hypercoordinate materials, greatly enriches the 2D family. Another example of theory-driven material design is graphane, which was computationally predicted[19] and later experimentally fabricated.[20]

The hotter topic in the scientific community is atomically thin materials with ferromagnetic properties. Recent theoretical predictions[21–43] and experimental syntheses[44–49] of ferromagnetic flat materials opened up new possibilities for their use in spintronic devices. Several years ago, it was theoretically predicted that a *cis*-semi-hydrated graphene sheet (*cis*-C_2H) is ferromagnetic.[50] By *ab initio* molecular dynamics, it was shown that this material is stable at room temperature and, therefore, is a promising structure for experimental synthesis. Inspired by that study, we decided to search for stable metal-free 2D materials with an unpaired p electron that would exhibit ferromagnetic properties. In our work we found that 2D SiN sheet is indeed ferromagnetic. Moreover, we showed that this novel material is dynamically and thermally stable, which makes SiN sheet a potential candidate for experimental synthesis.

2. Results and Discussion

Following the idea of finding ferromagnetic materials isoelectronic to semi-hydrated graphene, we tested three different compositions (C_2H, CN, SiN). Starting our research from the *trans*-semi-hydrogenated graphene (Figure S1a, Supporting Information) using the Solid-State Adaptive Natural Density Partitioning (SSAdNDP) method,[51–53] we found that the structure indeed has an unpaired p electron located on the unsaturated

N. V. Tkachenko, Prof. A. I. Boldyrev
Department of Chemistry and Biochemistry
Utah State University
Logan, UT 84322, USA
E-mail: a.i.boldyrev@usu.edu

Dr. B. Song, Prof. L.-M. Yang
Hubei Key Laboratory of Bioinorganic Chemistry and Materia Medica
Key Laboratory of Material Chemistry for Energy Conversion and Storage
Ministry of Education
Hubei Key Laboratory of Materials Chemistry and Service Failure
School of Chemistry and Chemical Engineering
Huazhong University of Science and Technology
Wuhan 430074, China

Dr. D. Steglenko, Prof. R. M. Minyaev
Institute of Physical and Organic Chemistry
Southern Federal University
194/2 Stachka Avenue, 344090 Rostov-on-Don, Russian Federation

ADVANCED
SCIENCE NEWS
www.advancedsciencenews.com

physica pssb
status solidi b
www.pss-b.com

carbon atom. However, it was shown that ferromagnetic coupling does not occur between two unpaired electrons. Moreover, calculated phonon dispersion curves indicate that $trans$-C_2H sheet is dynamically unstable, which makes this material impractical.

In the case of CN sheet (Figure S1b, Supporting Information), the analysis of electron density showed an unpaired p electron located on the carbon atom. However, no ferromagnetic coupling was observed. Replacing carbon atoms by silicon, we succeeded in obtaining ferromagnetic 2D SiN sheet (Figure S1c, Supporting Information), wherein the silicon atom carries a magnetic moment $1\mu_B$.

The SiN monolayer is not completely flat. It is a buckled 2D structure, where the relaxed bond length of Si–N is 1.770 Å, and z-axis distortion (distance between planes composed of Si and N) is 0.583 Å. For comparison, the relaxed CN plane is flatter with C–N bond length 1.389 Å and z-axis distortion 0.137 Å. The unit cell of SiN plane consists of one silicon and one nitrogen atom with lattice constants of $a = b = 2.894$ Å and belongs to the P_{3m1} space group (**Table 1**). The relaxed value of N–Si–N angle is 109.7°, which corresponds to the almost perfect angle between $sp3$-hybridized orbitals. To ensure that the structure with a ferromagnetic exchange is the minimum in energy, we calculated the total energy for nonmagnetic and antiferromagnetic states. It was shown that the ferromagnetic state of SiN sheet lies 0.122 eV per atom lower in energy than the nonmagnetic state, and 0.010–0.007 eV per atom lower than the two most stable antiferromagnetic states (Figure S3, Supporting Information). We believe that the geometric features and the more diffuse character of $3p$ orbitals, in comparison with $2p$ orbitals, provide the ferromagnetic properties of the SiN plane.
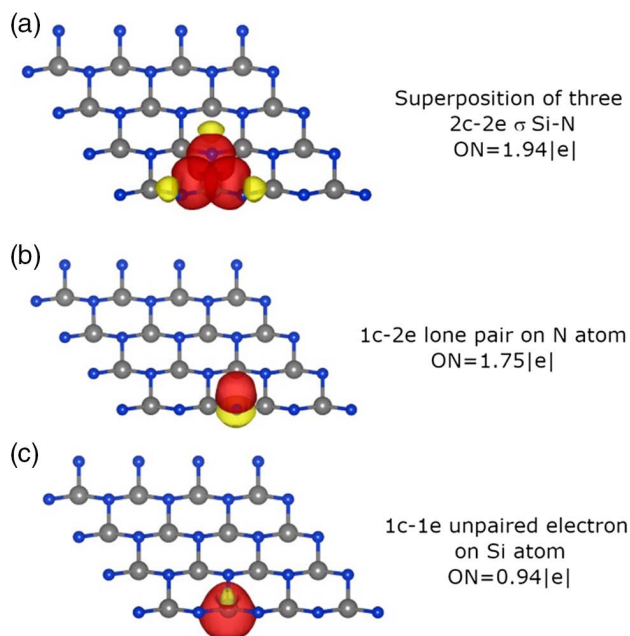
To understand the chemical bonding of the SiN sheet, we used the SSAdNDP method. We found that the bonding pattern could be described using only classical Lewis bonding elements such as two-center two-electron (2c–2e) bonds, lone pairs (1c–2e), and an unpaired electron (1c–1e) (**Figure 1**). We showed that occupation numbers (ONs) of SiN 2c–2e σ-bond (Figure 1a) and N 1c–2e lone pair (Figure 1b) are 1.94 |e| and 1.75 |e|, respectively. The occupancy of σ-bond is close to the ideal value 2.00 |e|, indicating the strong bonding interaction between Si and N atoms. The ON of 1c–1e $sp3$-hybridized orbital, responsible for the magnetic properties, is 0.94 |e| (Figure 1c).

The question of how to synthesize this material remains open now. Because of the presence of both unpaired electrons and lone pairs, the SiN sheet must be highly reactive. Thus, for experimental tests, it is worthwhile to conduct studies in a vacuum or inert atmosphere.
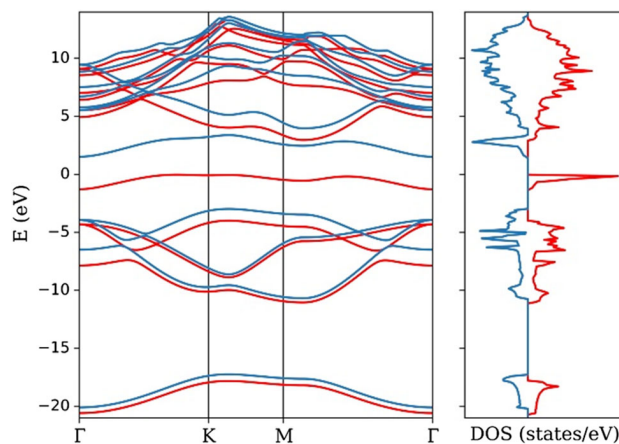
To understand the electronic properties of ferromagnetic SiN plane, we calculated its band structure and density of states (DOS), shown in **Figure 2**. For more accurate results, calculations were based on the screened hybrid functional of Heyd, Scuceria, and Ernzerhof (HSE06).[54,55] HSE06 is known to

Figure 1. Bonding structure of the SiN monolayer (silicon atoms are gray; nitrogen atoms are blue). The structure is presented at an angle. If we look from the top, the structure has C_{3v} local symmetry in the hexagon.

(a) Superposition of three 2c-2e σ Si–N ON=1.94|e|

(b) 1c-2e lone pair on N atom ON=1.75|e|

(c) 1c-1e unpaired electron on Si atom ON=0.94|e|

Figure 2. Band structure (left) and density of states (right) for the SiN monolayer calculated by the DFT PAW HSE06 method. The Fermi level was taken as zero. Red lines refer to spin-up states; blue lines refer to spin-down states. Γ (0, 0, 0), K (1/3, 2/3, 0), M (0, 1/2, 0) are special points in the first Brillouin zone.

yield accurate predictions of electronic bandgaps in semiconductors.[56] The SiN sheet has zero DOS at the Fermi level, which confirms the semiconductor properties of this material. It was shown that the indirect bandgap is 1.55 eV, though it is known that the standard DFT methods underestimate the bandgap. For comparison, the previously predicted two-layered 2D SiN is a semiconductor with a bandgap of 2.75 eV.[57] Note that the structural and electric properties of monolayered and two-layered SiN are different. This can be ascribed to the different types of interactions between the layers (covalent chemical

Table 1. Lattice constants, atomic positions, and total energy of ferromagnetic SiN sheet.

Atom	Atomic positions	a [Å]	b [Å]	c [Å]	E_{tot} [eV atom^{-1}]
Si	(0.000, 0.000, 0.481)	2.894	2.894	15.000	−6.894
N	(0.333, 0.667, 0.520)				

bonding interaction in case of two-layered SiN and van der Waals force in case of monolayered SiN).

The dynamic stability of the SiN sheet was tested by calculating the phonon dispersion spectrum (**Figure 3**) using a finite displacement method. We found that there are no low-frequency branches entering the imaginary region in the whole Brillouin zone, which is an evidence of the dynamic stability of this structure. The highest frequency mode reaches up to $850 \, cm^{-1}$, indicating strong Si–N interactions within the monolayer. The phonon density of states shows the contribution from each type of atoms and their relative weight.

To find the temperature conditions in which the SiN plane is stable, we performed *ab initio* Born-Oppenheimer molecular dynamics simulations. Simulations were calculated at different temperatures (20, 30, 100, 300, and 600 K) using a $4 \times 4 \times 1$ supercell. The time duration of simulation was 5 ps with a time step of 1 fs for all tests. Snapshots of the final structure, obtained at the end of each simulation, are shown in **Figure 4** and Figure S4, Supporting Information. We found that the structure is stable up to 600 K. However, due to the large fluctuations of the geometry and flipping of silicon atom to another side of the plane, the structure preserves ferromagnetic properties only at 20 K (Figure S2, Supporting Information). For higher temperatures, we found that the ferromagnetic state can only be stable during about 0.4 ps. After that time, the total magnetic moment becomes zero, i.e., magnetic quenching occurs. We should

mention that such a temperature does not correspond to the Curie temperature, since the simulation does not include spin dynamics. The obtained results indicate the stability of the magnetic state with respect to structural deformations.

3. Conclusions

In summary, we designed and computationally tested a novel 2D silicon mononitride material. It was shown that the ferromagnetic state of the SiN sheet is the most stable configuration in comparison with its nonmagnetic and antiferromagnetic states. The magnetic properties of the material can be described by the presence of ferromagnetically coupled unpaired p electrons sitting on the silicon atoms. Based on phonon spectrum and molecular dynamics simulations, we showed that the SiN sheet is dynamically and thermally stable. High-frequency modes show a strong Si–N interaction within the monolayer. We showed that the structure is stable up to 600 K and its ferromagnetic state is stable up to 20 K with respect to geometry fluctuations. The electronic structure indicates that this material is a semiconductor with an indirect bandgap of 1.55 eV. We believe that this material is of great interest to modern material science and will be experimentally obtained soon.
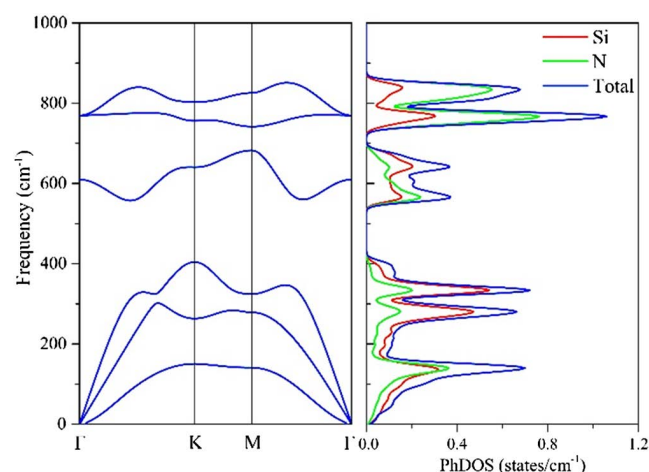
4. Computational Details

The details of computational methods can be found in the Supporting Information file.
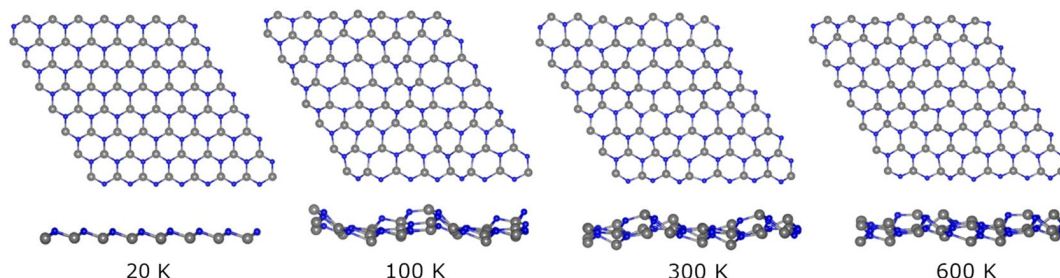
Supporting Information

Supporting Information is available from the Wiley Online Library or from the author.

Figure 3. Phonon dispersion and phonon density of states (PhDOS) of the SiN monolayer.

Figure 4. Top and side views of final frames ($2 \times 2 \times 1$ bounded supercell) of each molecular dynamics simulation test at different temperatures.

Conflict of Interest

The authors declare no conflict of interest.

Keywords

2D ferromagnets, silicon mononitride sheets, 2D semiconductors

[1] Special issue on "2D Materials Chemistry", *Chem. Rev.* **2018**, *118*, 6089–6456.
[2] Q. Tang, Z. Zhou, Z. Chen, *WIREs Comput. Mol. Sci.* **2015**, *5*, 360.
[3] D. Akinwande, N. Petrone, J. Hone, *Nat. Commun.* **2014**, *5*, 5678.
[4] D. Jariwala, V. K. Sangwan, L. J. Lauhon, T. J. Marks, M. C. Hersam, *ACS Nano* **2014**, *8*, 1102.
[5] A. Soumyanarayanan, N. Reyren, A. Fert, C. Panagopoulos, *Nature* **2016**, *539*, 509.
[6] K. S. Novoselov, A. K. Geim, S. V. Morozov, D. Jiang, M. I. Katsnelson, I. V. Grigorieva, S. V. Dubonos, A. A. Firsov, *Nature* **2005**, *438*, 197.
[7] K. S. Novoselov, A. K. Geim, S. V Morozov, D. Jiang, Y. Zhang, S. V. Dubonos, I. V. Grigorieva, A. A. Firsov, *Science* **2004**, *306*, 666.
[8] M. Martinez-Canales, T. R. Galeev, A. I. Boldyrev, C. J. Pickard, *Phys. Rev. B* **2017**, *96*, 195442.
[9] L. M. Yang, I. A. Popov, A. I. Boldyrev, T. Heine, T. Frauenheim, E. Ganz, *Phys. Chem. Chem. Phys.* **2015**, *17*, 17545.
[10] L. M. Yang, I. A. Popov, T. Frauenheim, A. I. Boldyrev, T. Heine, V. Bačić, E. Ganz, *Phys. Chem. Chem. Phys.* **2015**, *17*, 26043.
[11] L. M. Yang, V. Bačić, I. A. Popov, A. I. Boldyrev, T. Heine, T. Frauenheim, E. Ganz, *J. Am. Chem. Soc.* **2015**, *137*, 2757.
[12] B. Feng, B. Fu, S. Kasamatsu, S. Ito, P. Cheng, C. C. Liu, Y. Feng, S. Wu, S. K. Mahatha, P. Sheverdyaeva, P. Moras, M. Arita, O. Sugino, T. C. Chiang, K. Shimada, K. Miyamoto, T. Okuda, K. Wu, L. Chen, Y. Yao, I. Matsuda, *Nat. Commun.* **2017**, *8*, 1007.
[13] L. M. Yang, E. Ganz, *Phys. Chem. Chem. Phys.* **2016**, *18*, 17586.
[14] L. M. Yang, T. Frauenheim, E. Ganz, *J. Nanomater.* **2016**, *2016*, 8429510.
[15] L. M. Yang, T. Frauenheim, E. Ganz, *Phys. Chem. Chem. Phys.* **2015**, *17*, 19695.
[16] L. M. Yang, M. Dornfeld, T. Frauenheim, E. Ganz, *Phys. Chem. Chem. Phys.* **2015**, *17*, 26036.
[17] L. M. Yang, A. B. Ganz, M. Dornfeld, E. Ganz, *Condens. Matter* **2016**, *1*, 1.
[18] B. Song, Y. Zhou, H. M. Yang, J. H. Liao, L. M. Yang, X. B. Yang, E. Ganz, *J. Am. Chem. Soc.* **2019**, *141*, 3630.
[19] J. O. Sofo, A. S. Chaudhari, G. D. Barber, *Phys. Rev. B* **2007**, *75*, 153401.
[20] D. C. Elias, R. R. Nair, T. M. G. Mohiuddin, S. V. Morozov, P. Blake, M. P. Halsall, A. C. Ferrari, D. W. Boukhvalov, M. I. Katsnelson, A. K. Geim, K. S. Novoselov, *Science* **2009**, *323*, 610.
[21] Y. Li, Z. Zhou, S. Zhang, Z. Chen, *J. Am. Chem. Soc.* **2008**, *130*, 16739.
[22] Y. Li, Z. Zhou, P. Jin, Y. Chen, S. B. Zhang, Z. Chen, *J. Phys. Chem. C* **2010**, *114*, 12099.
[23] Q. Tang, Y. Li, Z. Zhou, Y. Chen, Z. Chen, *ACS Appl. Mater. Interfaces* **2010**, *2*, 2442.
[24] Y. Li, Z. Zhou, P. Shen, Z. Chen, *J. Phys. Chem. C* **2012**, *116*, 208.
[25] Q. Tang, F. Li, Z. Zhou, Z. Chen, *J. Phys. Chem. C* **2011**, *115*, 11983.
[26] F. Li, Z. Chen, *Nanoscale* **2013**, *5*, 5321.
[27] Z. Jiang, P. Wang, J. Xing, X. Jiang, J. Zhao, *ACS Appl. Mater. Interfaces* **2018**, *10*, 39032.
[28] M. Yu, X. Liu, W. Guo, *Phys. Chem. Chem. Phys.* **2018**, *20*, 6374.
[29] Q. Wu, J. J. Zhang, P. Hao, Z. Ji, S. Dong, C. Ling, Q. Chen, J. Wang, *J. Phys. Chem. Lett.* **2016**, *7*, 3723.
[30] L. Liu, S. Liu, Z. Zhang, W. Zhu, *J. Phys. Chem. C* **2017**, *121*, 24824.
[31] J. Liu, Q. Sun, Y. Kawazoe, P. Jena, *Phys. Chem. Chem. Phys.* **2016**, *18*, 8777.
[32] F. Wu, C. Huang, H. Wu, C. Lee, K. Deng, E. Kan, P. Jena, *Nano Lett.* **2015**, *15*, 8277.
[33] N. Sivadas, M. W. Daniels, R. H. Swendsen, S. Okamoto, D. Xiao, *Phys. Rev. B* **2015**, *91*, 235425.
[34] J. Liu, Q. Sun, *ChemPhysChem* **2014**, *16*, 614.
[35] V. V. Kulish, W. Huang, *J. Mater. Chem. C* **2017**, *5*, 8734.
[36] Z. Sun, H. Lv, Z. Zhuo, A. Jalil, W. Zhang, X. Wu, J. Yang, *J. Mater. Chem. C* **2018**, *6*, 1248.
[37] T. Zhao, J. Zhou, Q. Wang, Y. Kawazoe, P. Jena, *ACS Appl. Mater. Interfaces* **2016**, *8*, 26207.
[38] Z. Liu, J. Liu, J. Zhao, *J. Nano Res.* **2017**, *10*, 1972.
[39] C. S. Liu, X. L. Yang, J. Liu, X. J. Ye, *J. Phys. Chem. C* **2018**, *122*, 22137.
[40] Z. Jiang, P. Wang, X. Jiang, J. Zhao, *Nanoscale Horiz.* **2018**, *3*, 335.
[41] J. Zhou, Q. Sun, *J. Am. Chem. Soc.* **2011**, *133*, 15113.
[42] M. Kan, S. Adhikari, Q. Sun, *Phys. Chem. Chem. Phys.* **2014**, *16*, 4990.
[43] N. V. Tkachenko, D. Steglenko, N. Fedik, N. M. Boldyreva, R. M. Minyaev, V. I. Minkin, A. I. Boldyrev, *Phys. Chem. Chem. Phys.* **2019**, *21*, 19764.
[44] C. Gong, L. Li, Z. Li, H. Ji, A. Stern, Y. Xia, T. Cao, W. Bao, C. Wang, Y. Wang, Z. Q. Qiu, R. J. Cava, S. G. Louie, J. Xia, X. Zhang, *Nature* **2017**, *546*, 265.
[45] B. Huang, G. Clark, E. Navarro-Moratalla, D. R. Klein, R. Cheng, K. L. Seyler, D. Zhong, E. Schmidgall, M. A. McGuire, D. H. Cobden, W. Yao, D. Xiao, P. Jarillo-Herrero, X. Xu, *Nature* **2017**, *546*, 270.
[46] X. Zhang, J. Zhang, J. Zhao, B. Pan, M. Kong, J. Chen, Y. Xie, *J. Am. Chem. Soc.* **2012**, *134*, 11908.
[47] W. Xing, Y. Chen, P. M. Odenthal, X. Zhang, W. Yuan, T. Su, Q. Song, T. Wang, J. Zhong, S. Jia, *2D Mater.* **2017**, *4*, 024009.
[48] W. Cheng, J. He, T. Yao, Z. Sun, Y. Jiang, Q. Liu, S. Jiang, F. Hu, Z. Xie, B. He, W. Yan, S. Wei, *J. Am. Chem. Soc.* **2014**, *136*, 10393.
[49] K. Xu, P. Chen, X. Li, C. Wu, Y. Guo, J. Zhao, X. Wu, Y. Xie, *Angew. Chem. Int. Ed.* **2013**, *52*, 10477.
[50] J. Zhou, Q. Wang, Q. Sun, X. S. Chen, Y. Kawazoe, P. Jena, *Nano Lett.* **2009**, *9*, 3867.
[51] T. R. Galeev, B. D. Dunnington, J. R. Schmidt, A. I. Boldyrev, *Phys. Chem. Chem. Phys.* **2013**, *15*, 5022.
[52] D. Y. Zubarev, A. I. Boldyrev, *Phys. Chem. Chem. Phys.* **2008**, *10*, 5207.
[53] N. V. Tkachenko, A. I. Boldyrev, *Phys. Chem. Chem. Phys.* **2019**, *21*, 9590.
[54] J. Heyd, G. E. Scuseria, M. Ernzerhof, *J. Chem. Phys.* **2003**, *118*, 8207.
[55] J. Heyd, G. E. Scuseria, M. Ernzerhof, *J. Chem. Phys.* **2006**, *124*, 219906.
[56] J. Heyd, J. E. Peralta, G. E. Scuseria, R. L. Martin, *J. Chem. Phys.* **2005**, *123*, 174101.
[57] Y. Qian, Z. Du, R. Zhu, H. Wu, E. Kan, K. Deng, *EPL* **2018**, *122*, 47002.